Available online at www.sciencedirect.com

ScienceDirect

Mendeleev Commun., 2023, **33**, 314–317

Mendeleev Communications

New perylene diimide electron acceptors for organic electronics: synthesis, optoelectronic properties and performance in perovskite solar cells

Sergei A. Kuklin,*[a,b] Sergey V. Safronov,[a] Ekaterina A. Khakina,[a] Anastasiya G. Buyanovskaya,[a] Lyubov A. Frolova[b] and Pavel A. Troshin[b]

[a] *A. N. Nesmeyanov Institute of Organoelement Compounds, Russian Academy of Sciences, 119334 Moscow, Russian Federation. E-mail: ineos-50@mail.ru*

[b] *Federal Research Center of Problems of Chemical Physics and Medicinal Chemistry, Russian Academy of Sciences, 142432 Chernogolovka, Moscow Region, Russian Federation*

DOI: 10.1016/j.mencom.2023.04.005

Two new non-fullerene acceptors based on perylene diimide with acetylenic bridges were designed and synthesized employing Stille and Sonogashira coupling reactions as the key steps. Their optical and electronic properties were explored by UV–VIS spectroscopy and cyclic voltammetry, and energies of frontier molecular orbitals were estimated. Their preliminary studies in perovskite solar cells as electron transport materials showed the best power conversion efficiency for photocells of 14.18% value.

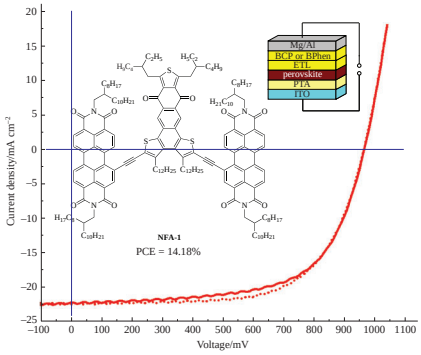

Keywords: perylene diimide, anthra[1,2-*b*:4,3-*b*′:6,7-*c*″]trithiophene, dithieno[2,3-*e*:3′,2′-*g*]isoindole, Stille coupling, Sonogashira coupling, PDI derivatives, small molecules, perovskite solar cells, electron transport materials.

In the past decade, the scientific direction that studies perovskite solar cells (PSCs) has been intensively developing, the achieved values of the power conversion efficiency (PCE) having been increased approximately from 3.8 to 25.5%.[1,2] To achieve a high PSC efficiency, it is important to provide the optimal microcrystalline structure of the light-absorbing perovskite layer, as well as the correspondence between the energy levels of the hole-transport (HTL) and electron-transport (ETL) layers as well as the uniformity and low defectiveness of films of the materials. In this case, the recombination of current carriers at the interlayer boundaries decreases and the balance of the electron and hole mobilities are achieved. Despite significant progress in increasing the efficiency, there is a problem of low stability of PSCs,[3] which prevents the further commercialization. One of the ways to solve the problem is the further development of new organic materials for charge-transport layers with optimized chemical structure.[4,5]

Perylene diimide (PDI) derivatives attract researchers' attention because they have a fairly developed π-electron system due to the presence of five fused benzene rings. Two additional annulated cycloimide moieties impart strong electron-withdrawing properties to the entire molecule, and the lowest unoccupied molecular orbital (LUMO) energy is usually in the range of –3.5 to –4.5 eV due to the presence of four electron-withdrawing carbonyl groups.[6] The fine tuning of electronic properties by the substituent variation provided good diversity of PDI derivatives. Many of them have been studied as non-fullerene acceptors (NFAs) in organic solar cells,[7–9] sensitive materials for fluorescent and colorimetric sensors,[10,11] electroluminescent compounds in organic light emitting diods[12] as well as materials for field-effect transistors.[13,14]

Recently, such compounds were used as charge-transport materials in PSCs. For example, for PSCs of various configurations with tetra-PDI derivative of tetraphenylethylene (TPE-PDI4) as an ETL layer, high efficiencies of 16.29 and 18.59% were observed. In addition, high hydrophobicity of TPE-PDI4 provides better protection of the perovskite layer from moisture as compared to $PC_{60}BM$, which can significantly increase the stability of photovoltaic cells.[15] Related phenothiazine dioxide derivatives (PDO-PDI2 and PDO-PDI3) in the PSCs based on mixed-halide perovskite provided an efficiency of 16.22 and 18.72%, respectively; at the same time, there was practically no *I*–*V* hysteresis and 93% of the initial efficiency was maintained for 720 h under accelerated aging conditions of non-encapsulated devices.[16] Incorporation of a (*N*,*N*-dimethylamino)alkyl PDI derivative (PDIN) with a very simple structure in p-i-n PSCs between Ag and $PC_{60}BM$ layers made it possible to increase the efficiency up to 17.00%, which was much higher than that of $PC_{60}BM$-only control devices (13.51%) under identical conditions.[17] For PSCs with ETL based on tetraaryloxy PDI derivatives, an efficiency of 16.8% was observed.[18] The use of $(PDI\text{-}C_6H_4)_2NPh$ (DPT) derivative with a central fragment based on a double-substituted triphenylamine in PSCs allowed one to achieve a PCE of 20.07% with negligible hysteresis during forward and reverse scans, which can be attributed to a suppressed ion migration in perovskite and charge accumulation at the interface between perovskite and ETL.[19]

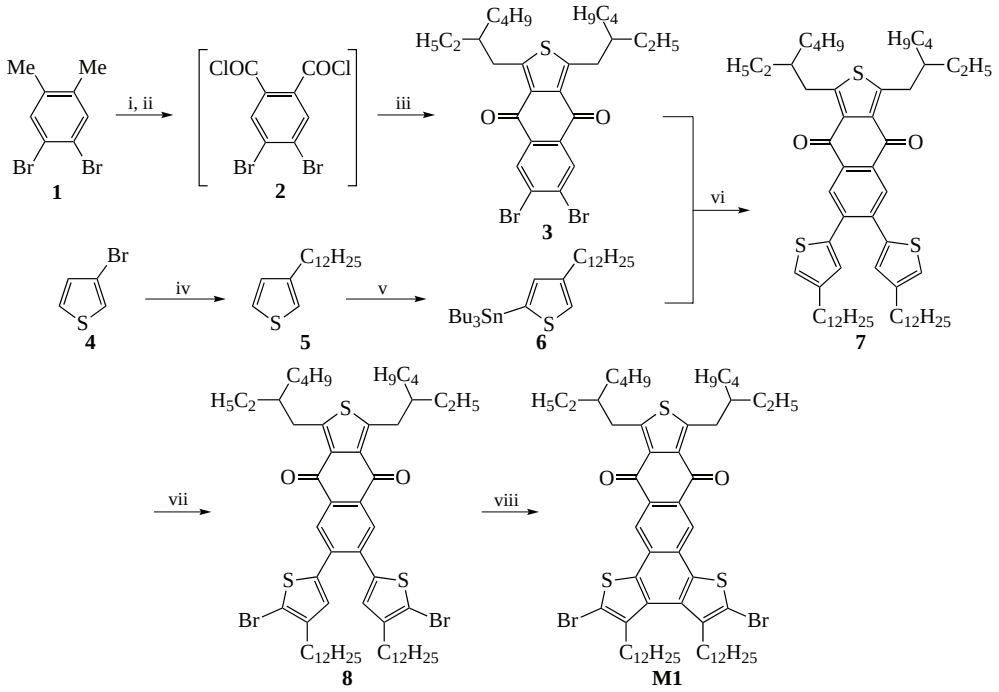

Scheme 1 *Reagents and conditions*: i, $KMnO_4$, H_2O, reflux, 6 h; ii, $(COCl)_2$, CH_2Cl_2/DMF, reflux, 24 h; iii, 2,5-bis(2-ethylhexyl)thiophene, $AlCl_3$, 0...25 °C, 24 h; iv, *n*-$C_{12}H_{25}MgBr$, $NiCl_2$(dppp), THF, reflux, 16 h; v, LDA, THF, –80...0 °C, then $ClSnBu_3$, THF, –80...25 °C; vi, $Pd(PPh_3)_4$, toluene, reflux, 24 h; vii, NBS, CH_2Cl_2/AcOH (3 : 1), 0...25 °C, 24 h; viii, $FeCl_3$, CH_2Cl_2/$MeNO_2$, 25 °C, 10 h.

In this work, we synthesized new structural blocks **M1** and **M2** based on anthra[1,2-*b*:4,3-*b*′:6,7-*c*″]trithiophene-8,12-dione and dithieno[2,3-*e*:3′,2′-*g*]isoindole-7,9(8*H*)-dione, respectively, and used them as substituents in the PDI fragments, attaching them through acetylene bridges (Schemes 1 and 2). The resulting new non-fullerene acceptors (NFAs) **NFA-1** and **NFA-2** (Scheme 3) were fully characterized and tested as ETL materials in PSCs and an efficiency of 14.18% was observed with open-circuit voltage (V_{oc}) of 960.33 mV, short-circuit current density (J_{sc}) of 22.78 mA cm^{-2}, and filling factor (FF) of 64.84%. The obtained results show that **NFA-1** is a promising compound for further structural optimization for operation in perovskite solar cells.

New monomer of anthra[1,2-*b*:4,3-*b*′:6,7-*c*″]trithiophene series **M1** was synthesized as outlined in Scheme 1. The key step was the Friedel–Crafts acylation of 2,5-bis(2-ethylhexyl)-thiophene with 4,5-dibromophthaloyl dichloride **2** which led to tricyclic compound **3** with a satisfactory yield of about 40%. Its further Stille reaction with tributyl(4-dodecylthiophen-2-yl)-stannane **6** followed by bromination afforded compound **8** in 71% yield. Final oxidative cyclization of **8** with $FeCl_3$ gave the target monomer **M1** in 60% yield.

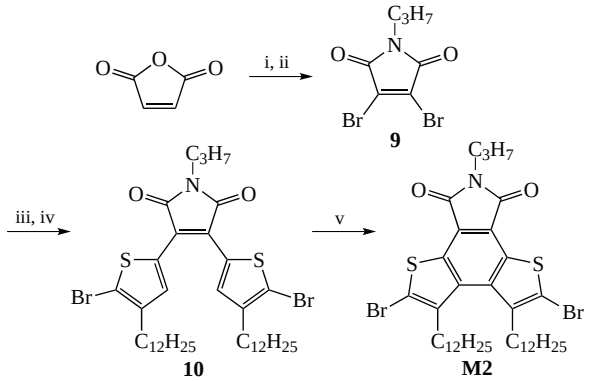

Scheme 2 *Reagents and conditions*: i, *n*-$C_3H_7NH_2$, THF, 0...20 °C, 1 h, then KOAc, $(EtCO)_2O$, room temperature, 24 h; ii, Br_2, AcOH, 80 °C, 16 h; iii, stannane **6**, $Pd(PPh_3)_4$, toluene, reflux, 16 h; iv, NBS, CH_2Cl_2/AcOH (2 : 1), 0...20 °C, 16 h; v, UV 465 nm, I_2, O_2 (air), toluene.

Another new monomer of dithieno[2,3-*e*:3′,2′-*g*]isoindole type **M2** was obtained in several stages from maleic anhydride (see Scheme 2), with the principal steps being analogous to the preparation of **M1** (see Scheme 1). The final oxidative cyclization of intermediate **10** was performed, however, with atmospheric oxygen upon irradiation with 465 nm light.

The new monomeric fragments **M1** and **M2** look promising for designing new materials for organic electronics. Electrochemically estimated LUMO energies of **M1**, **M2** are of –2.80 and –2.87 eV, respectively; absorption edges located at 448 and 467 nm correspond to the optical bandgap (E_g^{opt}) values of 2.77 and 2.66 eV (Figure 1). The HOMO level energies estimated from these data are of –5.57 and –5.53 eV for **M1** and **M2** (Table 1). Thus, compounds **M1** and **M2** have weak electron-acceptor nature due to the presence of quinone and cyclic imide rings in the structures, respectively.

Monomers **M1** and **M2** were readily functionalized with trimethylsilylacetylene in the Sonogashira reaction followed by desilylation to form diethynyl intermediates **11** and **12** (see Scheme 3). These compounds were coupled with PDI-Br precursor **13** under the Sonogashira conditions to afford new bis-PDI compounds **NFA-1** and **NFA-2**. Both of them were also prepared in moderate yields using one-pot desilylation–Sonogashira coupling procedure as reported recently[20] (see Online Supplementary Materials).

Both compounds **NFA-1** and **NFA-2** have high absorption coefficients in the entire visible spectrum [Figure 1(*a*)] due to strong intramolecular charge transfer from donor central fragments to PDI electron-withdrawing groups. The absorption edges of compounds locate at 653 and 668 nm, which corresponds to E_g^{opt} values of 1.90 and 1.85 eV for **NFA-1** and **NFA-2**, respectively (see Table 1).

The LUMO energies of both acceptors **NFA-1** and **NFA-2**, estimated from CVA curves, are practically equal (–3.86 eV); the corresponding HOMO energies are of –5.73 and –5.71 eV, respectively [see Figure 1(*c*) and Table 1]. These values are very close to the E_{HOMO}/E_{LUMO} values for the well-known PDI acceptors Fluorene-PDI2 (–6.18/–3.95 eV),[21] TPE-PDI4 (–5.82...–5.89/–3.77...–3.78 eV),[15,22] Spirobifluorene-PDI2

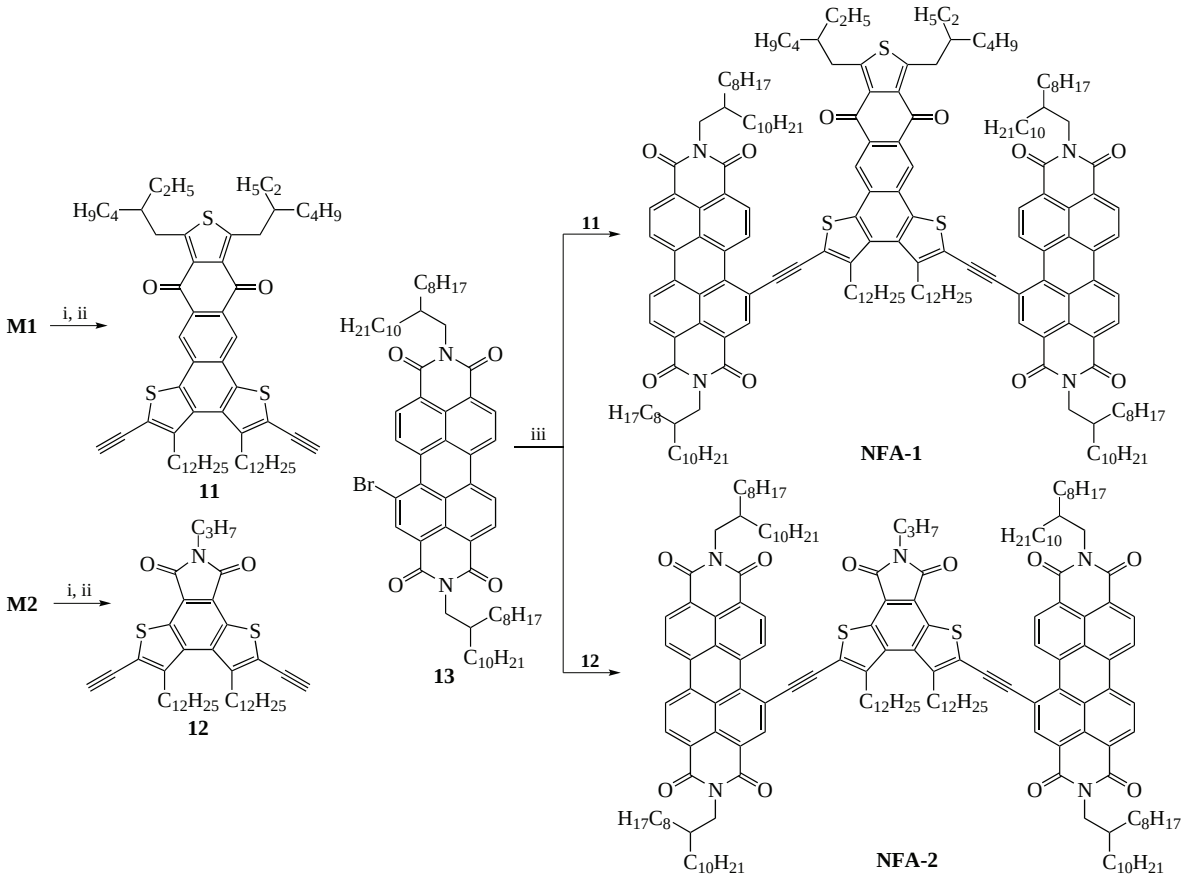

Scheme 3 *Reagents and conditions*: i, $Me_3SiC{\equiv}CH$, $PdCl_2(PPh_3)_2$, PPh_3, CuI, THF/NEt_3 (1 : 1); ii, $KF/MeOH/H_2O$; iii, $PdCl_2(PPh_3)_2$, PPh_3, CuI, NEt_3.

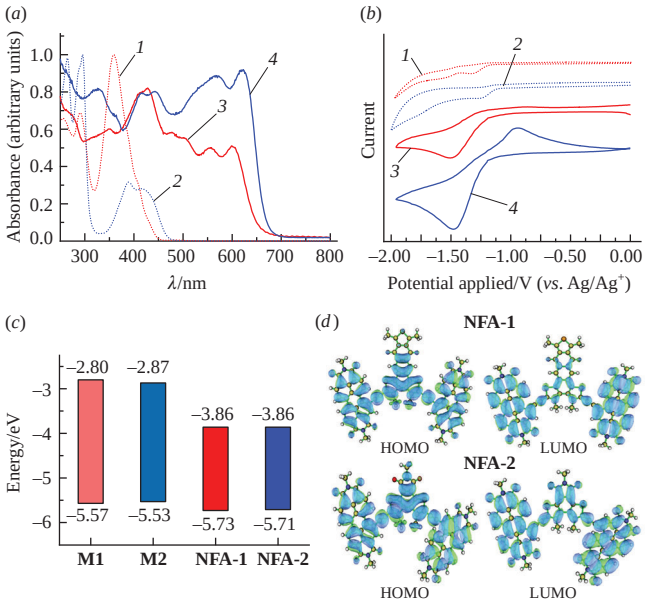

Figure 1 (*a*) Absorption spectra, (*b*) cyclic voltammograms of films, (*c*) energy level diagram and (*d*) calculated HOMO/LUMO distribution for (*1*) **M1**, (*2*) **M2**, (*3*) **NFA-1** and (*4*) **NFA-2**.

Table 1 Optical and electronic properties of **M1**, **M2**, **NFA-1** and **NFA-2**.

Compound	λ_{ons}[a]/nm	E_g^{opt}[b]/eV	E_{ons}^{red}[c]/V	E_{LUMO}[d]/eV	E_{HOMO}[e]/eV	E_{LUMO}^{T}[f]/eV	E_{HOMO}^{T}[f]/eV
M1	448	2.77	–1.683	–2.80	–5.57	–2.87	–6.22
M2	467	2.66	–1.613	–2.87	–5.53	–2.97	–6.21
NFA-1	653	1.90	–1.190	–3.86	–5.73	–3.80	–5.88
NFA-2	668	1.85	–1.192	–3.86	–5.71	–3.87	–5.86

[a] In film casted from $CHCl_3$. [b] $E_g^{opt} = 1240/\lambda_{ons}$. [c] In 0.1 M $Bu_4NPF_6/MeCN$, Pt working electrode, Ag/AgCl reference electrode, scanning rate 100 mV s^{-1}. [d] $E_{LUMO} = -e(E_{ons}^{red} + 4.48)$, where 4.48 eV is the HOMO energy of ferrocene. [e] $E_{HOMO} = E_{LUMO} - E_g^{opt}$. [f] Calculated on B3LYP//6-311++G(d,p) level of theory.

(SF-PDI2) (–5.82/–3.80 eV),[23] triphenylphosphine derivatives PPh_3-PDI3, PPh_3O-PDI3, PPh_3S-PDI3 (–5.85/–3.64, −5.88/−3.70 and −5.89/−3.74 eV, respectively),[24] TPDI, ThPDI and O-PDI (−5.68/−3.77, −5.71/−3.76 and −5.73/−3.80 eV, respectively).[25] The DFT calculated E_{HOMO}/E_{LUMO} values for compounds **NFA-1** and **NFA-2** are of –5.88/–3.80 and –5.86/–3.87 eV, respectively (see Table 1), and are in a good agreement with the experimental data. The HOMO and LUMO distributions within the **NFA-1** and **NFA-2** molecules are shown in Figure 1(*d*) (see also Online Supplementary Materials, Figures S8 and S9). Visually, in the **NFA-1** molecule HOMO is fairly uniformly distributed throughout the entire molecule, and the LUMO orbital is mainly localized on the terminal PDI fragments. A similar picture is observed for **NFA-2**. From the data obtained one may conclude that **NFA-1** and **NFA-2** are promising electron acceptor compounds and can be used in organic and hybride electronic devices.

In this work we studied **NFA-1** and **NFA-2** in inverted perovskite photovoltaic cells as electron-transport materials. The structure of PSCs was ITO/PTA/$MAPbI_3$/**ETL**/HBL/Mg/Al, (ITO is indium tin oxide; BCP is bathocuproine; BPhen is bathophenanthroline), where HBL is additional hole-blocking layer such as BCP (5 nm), BPhen (5 nm) or WO_3 (15 nm). We did not observe significant efficiency of PSCs with ETL = = **NFA-2** (the best PCE is only of 3.36% at V_{oc} = 1003.74 mV, J_{sc} = 14.25 mA cm^{-2}, and FF = 23.44%). But when **NFA-1** was used as ETL, we observed promising PCE values up to 13.44% at V_{oc} = 903.35 mV, J_{sc} = 22.20 mA cm^{-2} and FF = 67.01% for the PCSs with the structure ITO/PTA/$MAPbI_3$/**NFA-1**/BCP/Mg/Al. When using BPhen as a hole-blocking material, the

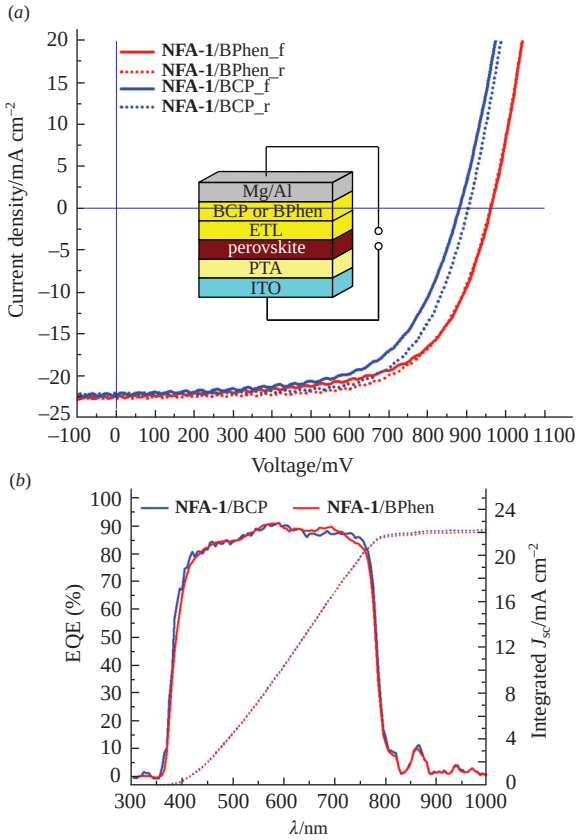

Figure 2 (*a*) Structure and *J*–*V* characteristics and (*b*) EQE spectra of the PSCs with **NFA-1** as ETLs.

Table 2 Parameters of PSCs with **NFA-1** in ETL composition.

ETL[a]	Scan direction	V_{oc}/ mV	J_{sc}/ mA cm^{-2}	FF (%)	PCE (%)	$J_{sc\ EQE}$[b]/ mA cm^{-2}
NFA-1/BCP (5 nm)	F	881.09	22.41	61.98	12.24	22.09
	R	903.35	22.20	67.01	13.44	
NFA-1/BPhen (5 nm)	F	961.47	22.47	63.81	13.79	21.97
	R	960.33	22.78	64.84	14.18	

[a] PSCs with the ITO/PTA/perovskite/**NFA-1**/BCP or BPhen/Mg/Al structure were studied under illumination with a standard light source AM1.5 (100 mW), cell area was 0.08 cm^2. [b] $J_{sc\ EQE}$ was the short circuit current density calculated by integrating the EQE spectrum.

PSCs efficiency slightly increased up to 14.18% at V_{oc} = 960.33 mV, J_{sc} = 22.78 mA cm^{-2} and FF = 64.84%. Basically, this growth is due to the increase in V_{oc} by 60–80 mV when using BPhen [Figure 2(*a*) and Table 2].

In both PSCs configurations, the external quantum yield (EQE) exceeds 80% in the visible wavelength range of 420–770 nm [Figure 2(*b*)]. The maximum EQE values for both structures are of 90% at 580 nm. The short circuit current values obtained by integrating the EQE spectra are 22.09 and 21.97 mA cm^{-2}, which is in good agreement with the values obtained by measuring the current–voltage characteristics (see Table 2).

In conclusion, two new monomers **M1** and **M2** based on anthra[1,2-*b*:4,3-*b*′:6,7-*c*″]trithiophene-8,12-dione and dithieno[2,3-*e*:3′,2′-*g*]isoindole-7,9(8*H*)-dione were designed and synthesized. They were used for the preparation of new perylene diimide derivatives, **NFA-1** and **NFA-2**, with acetylenic bridges. The optical and electronic properties of the new compounds were studied by UV–VIS spectroscopy and cyclic voltammetry, and HOMO/LUMO energy levels were estimated. Compounds **NFA-1** and **NFA-2** were preliminarily examined in perovskite solar cells (PSCs) as electron transport materials (ETM). The best power conversion efficiency (PCE) for PSCs with ETM = = **NFA-1** was of 14.18%. The obtained results show that **NFA-1** is a promising compound for further structural optimization for operation in perovskite solar cells.

This study was funded by the Russian Science Foundation (grant no. 22-23-00318). NMR, MALDI-TOF MS, UV-absorption, cyclic voltammetry studies and elemental analysis were performed with the financial support of the Ministry of Science and Higher Education of the Russian Federation employing the equipment of Center for molecular composition studies of INEOS RAS.

Online Supplementary Materials

Supplementary data associated with this article can be found in the online version at doi: 10.1016/j.mencom.2023.04.005.

References

1 A. Kojima, K. Teshima, Y. Shirai and T. Miyasaka, *J. Am. Chem. Soc.*, 2009, **131**, 6050.
2 G. Ren, W. Han, Y. Deng, W. Wu, Z. Li, J. Guo, H. Bao, C. Liu and W. Guo, *J. Mater. Chem. A*, 2021, **9**, 4589.
3 L. Meng, J. You and Y. Yang, *Nat. Commun.*, 2018, **9**, 5265.
4 B. Li and W. Zhang, *Commun. Mater.*, 2022, **3**, 65.
5 V. A. Kabanova, O. L. Gribkova, A. R. Tameev and A. A. Nekrasov, *Mendeleev Commun.*, 2021, **31**, 454.
6 B. A. Jones, A. Facchetti, M. R. Wasielewski and T. J. Marks, *J. Am. Chem. Soc.*, 2007, **129**, 15259.
7 V. Sharma, J. D. B. Koenig and G. C. Welch, *J. Mater. Chem. A*, 2021, **9**, 6775.
8 Y. Duan, X. Xu, Y. Li and Q. Peng, *Chin. Chem. Lett.*, 2017, **28**, 2105.
9 J. Hou, O. Inganäs, R. H. Friend and F. Gao, *Nat. Mater.*, 2018, **17**, 119.
10 S. Ali, A. Gupta, M. Shafiei and S. J. Langford, *Chemosensors*, 2021, **9**, 30.
11 S. Chen, Z. Xue, N. Gao, X. Yang and L. Zang, *Sensors*, 2020, **20**, 917.
12 L. Zong, Y. Gon, Y. Yu, Y. Xie, G. Xie, Q. Peng, Q. Li and Z. Li, *Sci. Bull.*, 2018, **63**, 108.
13 P. Cheng, X. Zhao and X. Zhan, *Acc. Mater. Res.*, 2022, **3**, 309.
14 W. V. Wang, Y. Zhang, X.-Y. Li, Z.-Z. Chen, Z.-H. Wu, L. Zhang, Z.-W. Lin and H.-L. Zhang, *InfoMat*, 2021, **3**, 814.
15 K. Jiang, F. Wu, H. Yu, Y. Yao, G. Zhang, L. Zhu and H. Yan, *J. Mater. Chem. A*, 2018, **6**, 16868.
16 M. Zheng, Y. Miao, A. A. Syed, C. Chen, X. Yang, L. Ding, H. Li and M. Cheng, *J. Energy Chem.*, 2021, **56**, 374.
17 J. Miao, Z. Hu, M. Liu, M. U. Ali, O. Goto, W. Lu, T. Yang, Y. Liang and H. Meng, *Org. Electron.*, 2018, **52**, 200.
18 G. S. Perez, S. Dasgupta, W. Żuraw, R. F. Pineda, K. Wojciechowski, L. K. Jagadamma, I. Samuel and N. Robertson, *J. Mater. Chem. A*, 2022, **10**, 11046.
19 Y. Fan, F. Wu, F. Liu, M. Han, K. Chang, L. Zhu, Q. Li and Z. Li, *J. Mater. Chem. C*, 2022, **10**, 2544.
20 J. S. Capani, J. E. Cochran and J. Liang, *J. Org. Chem.*, 2019, **84**, 9378.
21 M. L. Keshtov, S. A. Kuklin, I. O. Konstantinov, I. E. Ostapov, Z. Xie, E. N. Koukaras, R. Suthare and G. D. Sharma, *Sol. Energy*, 2020, **205**, 211.
22 M. L. Keshtov, S. A. Kuklin, I. E. Ostapov, M. I. Buzin, V. G. Alekseev, P. V. Komarov, C. Dou, H. Dahiya and G. D. Sharma, *Opt. Mater.*, 2021, **115**, 111048.
23 K. Jiang, G. Zhang, G. Yang, J. Zhang, Z. Li, T. Ma, H. Hu, W. Ma, H. Ade and H. Yan, *Adv. Energy Mater.*, 2017, **8**, 1701370.
24 G. Zhang, J. Feng, X. Xu, W. Ma, Y. Li and Q. Peng, *Adv. Funct. Mater.*, 2019, **29**, 1906587.
25 Y. Gong, K. Chang, C. Chen, M. Han, X. Zhan, J. Min, X. Jiao, Q. Li and Z. Li, *Mater. Chem. Front.*, 2019, **3**, 93.

Received: 30th November 2022; Com. 22/7055